Mon. Not. R. Astron. Soc. **392,** 1532–1538 (2009) doi:10.1111/j.1365-2966.2008.14178.x

WASP-14b: 7.3 M_J transiting planet in an eccentric orbit

Y. C. Joshi,[1⋆] D. Pollacco,[1] A. Collier Cameron,[2] I. Skillen,[3] E. Simpson,[1] I. Steele,[4] R. A. Street,[5] H. C. Stempels,[2] D. J. Christian,[1] L. Hebb,[2] F. Bouchy,[6] N. P. Gibson,[1] G. Hébrard,[6] F. P. Keenan,[1] B. Loeillet,[6,7] J. Meaburn,[8] C. Moutou,[7] B. Smalley,[9] I. Todd,[1] R. G. West,[10] D. R. Anderson,[9] S. Bentley,[9] B. Enoch,[11] C. A. Haswell,[11] C. Hellier,[9] K. Horne,[2] J. Irwin,[12] T. A. Lister,[5] I. McDonald,[9] P. Maxted,[9] M. Mayor,[13] A. J. Norton,[11] N. Parley,[11] C. Perrier,[14] F. Pont,[15] D. Queloz,[13] R. Ryans,[1] A. M. S. Smith,[2] S. Udry,[13] P. J. Wheatley[16] and D. M. Wilson[9]

[1]*Astrophysics Research Centre, School of Mathematics and Physics, Queen's University, University Road, Belfast BT7 1NN*
[2]*School of Physics and Astronomy, University of St Andrews, North Haugh, St Andrews, Fife KY16 9SS*
[3]*Isaac Newton Group of Telescopes, Apartado de Correos 321, E-38700 Santa Cruz de la Palma, Tenerife, Spain*
[4]*Astrophysics Research Institute, Liverpool John Moores University, Twelve Quays House, Egerton Wharf, Birkenhead CH41 1LD*
[5]*Las Cumbres Observatory, 6740 Cortona Dr. Suite 102, Santa Barbara, CA 93117, USA*
[6]*Institut d'Astrophysique de Paris, UMR 7095 CNRS, Université Pierre and Marie Curie, 98bis bvd. Arago, 75014 Paris, France*
[7]*Laboratoire d'Astrophysique de Marseille, CNRS (UMR 6110), BP8, 13376 Marseille Cedex 12, France*
[8]*Department of Physics and Astronomy, University of Manchester, Manchester, Macclesfield, Cheshire, SK11 9DL*
[9]*Astrophysics Group, Keele University, Staffordshire ST5 5BG*
[10]*Department of Physics and Astronomy, University of Leicester, Leicester, LE1 7RH*
[11]*Department of Physics and Astronomy, The Open University, Milton Keynes, MK7 6AA*
[12]*Harvard-Smithsonian Center for Astrophysics, 60 Garden Street MS-16, Cambridge, MA 02138-1516, USA*
[13]*Observatoire de Genève, Université de Genève, 51 Ch. des Maillettes, 1290 Sauverny, Switzerland*
[14]*Laboratoire d'AstrOphysique, Observatoire de Grenoble, Univ. J. Fourier - BP 53, F-38041 Grenoble Cedex 9, France*
[15]*Physikalisches Institu, University of Bern, Sidlerstrass 5, 3012 Bern, Switzerland*
[16]*Department of Physics, University of Warwick, Coventry CV4 7AL*

Accepted 2008 October 31. Received 2008 October 29; in original form 2008 September 10

ABSTRACT

We report the discovery of a 7.3 M_J exoplanet WASP-14b, one of the most massive transiting exoplanets observed to date. The planet orbits the 10th-magnitude F5V star USNO-B1 11118−0262485 with a period of 2.243 752 d and orbital eccentricity $e = 0.09$. A simultaneous fit of the transit light curve and radial velocity measurements yields a planetary mass of 7.3 ± 0.5 M_J and a radius of 1.28 ± 0.08 R_J. This leads to a mean density of about 4.6 g cm^{-3} making it the densest transiting exoplanets yet found at an orbital period less than 3 d. We estimate this system to be at a distance of 160 ± 20 pc. Spectral analysis of the host star reveals a temperature of 6475 ± 100 K, $\log g = 4.07$ cm s^{-2} and $v \sin i = 4.9 \pm 1.0$ km s^{-1}, and also a high lithium abundance, $\log N(\mathrm{Li}) = 2.84 \pm 0.05$. The stellar density, effective temperature and rotation rate suggest an age for the system of about 0.5–1.0 Gyr.

Key words: techniques: photometric – techniques: radial velocities – stars: individual: GSC 01482−00882.

1 INTRODUCTION

The giant exoplanets that transit across the discs of their host stars are of great interest due to their impact on our understanding of planetary structure. Since the first discovery of a transiting exoplanet HD 209458b (Charbonneau et al. 2000; Henry et al. 2000), more than 40 transiting systems have been found around nearby stars. Transit light curves, along with their radial velocity (RV) motions, provide a wealth of information about the system including precise mass, radius and mean density of the planet. This in turn allows us to probe their internal structure by comparing their physical parameters with the models of planetary structure and evolution (Guillot et. al 2006; Fortney, Marley & Barnes 2007). Given the importance of these systems, several wide-field surveys are in progress to find the transiting exoplanets, e.g. HAT (Bakos et al. 2004), XO

⋆E-mail: y.joshi@qub.ac.uk

(McCullough et al. 2005), TrES (O'Donovan et al. 2006) and SuperWASP (Pollacco et al. 2006).

In this paper, we report the 14th exoplanet discovered in the SuperWASP survey which is orbiting around a 10th-magnitude F5-type star in the Northern Hemisphere. This paper is organized as follows. In Section 2, we give details of the discovery light curve and outcome of our follow-up photometric and spectroscopic observations. Spectral analysis to determine system parameters is described in Section 3. The stellar and planetary evolutionary status is discussed in Section 4. Finally, our results are briefly summarized in Section 5.

2 OBSERVATIONS

2.1 SuperWASP observations

WASP-14 (=1SWASPJ143306.35+215340.9 = USNO-B1 1118−0262485 = GSC 01482−00882) is an F5V star with $V = 9.75$ and $B - V = 0.46$ in the constellation Boötes. It was monitored by the SuperWASP instrument on La Palma during 2004 May to 2007 June. A detailed description of the SuperWASP instrument, observing procedure and data-processing issues is given in Pollacco et al. (2006), while a discussion of the candidate-selection procedure is explained in Collier Cameron et al. (2006, 2007). A total of 7338 data points were obtained for this star in four observing runs and in two different cameras. The SuperWASP discovery light curve of WASP-14b, as shown in Fig. 1, reveals a transit recurring with a period of 2.243 752 d and a total duration of about 180 min between the first and fourth contact.

2.2 Photometric follow-up

Initial follow-up photometric observations of WASP-14 were carried out by Las Cumbres Observatory, S. Arizona's 81-cm Tenagra robotic telescope and Keele University Observatory 60-cm telescope in *I* and *R* bands, respectively. All the images were bias-subtracted and flat-fielded before doing aperture photometry around bright stars. Light curves along with the SuperWASP discovery data around the transit phase are shown together with model fits in Fig. 2(a).

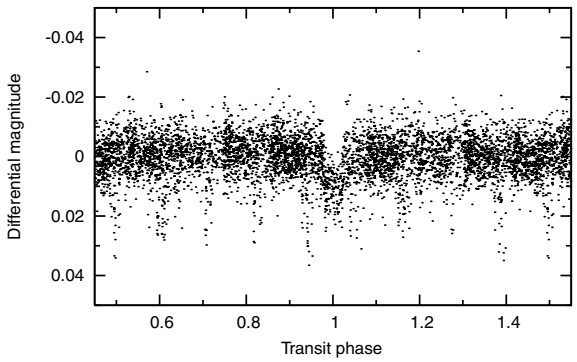

Figure 1. The SuperWASP discovery light curve for the WASP-14 (1SWASPJ143306.35+215340.9). The data points are phased using the ephemeris, T_0(HJD) = 245 4463.575 83, and folded on the orbital period of 2.243 752 d.

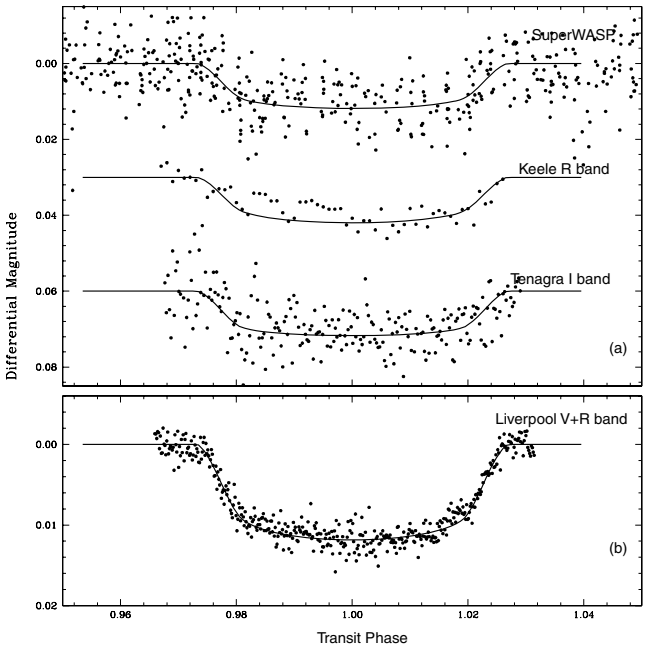

Figure 2. (a) Phase-folded transit light curves from the SuperWASP, Tenagra and Keele data. (b) A high-precision transit light curve of WASP-14 observed with the *RISE*. The best-fitting model curves determined from a simultaneous MCMC fit (see detail in Section 3.3) are shown by the solid lines.

In order to obtain a higher precision photometry[1] of WASP-14, we observed the target field using the high-speed imaging camera *RISE* mounted on the robotic 2-m Liverpool Telescope (Gibson et al. 2008; Steele et al. 2008). We observed the transit on the night of 2008 May 04 in a single broad-band $V + R$ filter as part of the Canarian Observatories *International Time Programme*. The *RISE* Camera consists of a thermoelectrically cooled 1024 × 1024 pixel CCD detector which has a pixel scale of ∼0.55 arcsec pixel^{-1} and a total field of view of ∼9.4 × 9.4 arcmin^2. During this period, we obtained 7200 frames of 2-s exposures in 2 × 2 spatial binning. Aperture photometry was performed using the IRAF DAOPHOT routine around the target and three bright, non-variable comparison stars using an aperture of radius 8 pixels. We binned the images in 30-s blocks to increase signal-to-noise ratio (S/N). To derive the differential magnitude of WASP-14, we produced a ratio of the combined flux from the comparison stars to that from WASP-14. We modelled the transit light curve using a Markov chain Monte Carlo (MCMC) algorithm (see Section 3.3). The resulting normalized transit light curve of WASP-14 along with a model fit is shown in Fig. 2(b). From the model fit, we estimated a transit depth of about 12 mmag $[(R_P/R_*)^2 = 0.0102]$ and a rms residuals of 1.4 mmag around the best fit.

2.3 Spectroscopic follow-up

To derive the orbital parameters of the planetary system, we obtained spectroscopic observations with the FIbre-fed Echelle Spectrograph (FIES) mounted on the 2.5-m Nordic Optical Telescope. A total of six high-resolution spectra of WASP-14 with an exposure time of 900 s covering the wavelength region 4000–7350 Å were obtained

[1] The data is available upon request.

Table 1. RVs for WASP-14 from FIES/NOT and SOPHIE/OHP data. The first six data points were taken from FIES instrument while the others were obtained with SOPHIE.

Time (BJD 245 0000)	RV ($km\,s^{-1}$)	σ_{RV} ($km\,s^{-1}$)	Bis span ($km\,s^{-1}$)[a]
4461.7400	−5.8705	0.0080	0.0667
4462.7710	−4.1180	0.0054	0.0629
4465.7490	−4.8489	0.0078	0.0332
4466.7850	−5.4037	0.0044	0.0388
4490.7700	−5.6209	0.0087	0.0392
4490.7820	−5.6383	0.0081	−0.0069
4508.5938	−5.3563	0.0112	0.0410
4509.5238	−5.0654	0.0114	0.0070
4509.5830	−4.8313	0.0098	0.0270
4510.5074	−4.5874	0.0129	0.0540
4510.5599	−4.7205	0.0106	0.0330
4510.6509	−4.8798	0.0099	0.0260
4510.6569	−4.8954	0.0107	0.0110
4510.6630	−4.9138	0.0111	0.0670
4510.6860	−4.9758	0.0100	0.0130
4510.7215	−5.0906	0.0108	0.0320
4510.7274	−5.1086	0.0112	0.0390
4511.5572	−5.6865	0.0107	0.0200
4511.6822	−5.3425	0.0114	0.0370
4512.5406	−4.2173	0.0109	0.0220
4512.5682	−4.2696	0.0125	0.0250
4512.6822	−4.4391	0.0107	0.0530
4512.7152	−4.5081	0.0103	0.0580
4515.6212	−5.8950	0.0099	−0.0070
4518.6525	−4.5850	0.0117	0.0340
4524.6750	−5.9753	0.0107	0.0700
4525.6755	−4.0564	0.0091	0.0560

[a]Bisector spans; $\sigma_{BS} \approx 2.5\,\sigma_{RV}$.

during 2007 December 27–31 and 2008 January 25. A further 21 RV points were secured using the SOPHIE spectrograph on the 1.93-m telescope at observatoire de Haute-Provence during 2008 February 12–16, plus one point each on the nights of 2008 February 19, 22, 28 and 29. A detailed description about the FIES and SOPHIE observations is given in Christian et al. (2008). The journal of the FIES and SOPHIE observations is given in Table 1, and includes barycentric Julian dates (BJD), RV measurements and associated error. A phase-folded RV curve overplotted with the maximum-likelihood orbit model is shown in the upper panel of Fig. 3(a). This shows RV variations with a semi-amplitude $K_1 = 0.993\,km\,s^{-1}$ and the period derived from the photometric observations. The velocity rms to the orbital fit for FIES and SOPHIE are 5.8 and 11.0 $m\,s^{-1}$, respectively.

The variation of the line bisector with orbital phase is often used as a tool to detect blended stellar companions or chromospheric activity (Queloz et al. 2001). From the CCF, we obtained the line bisector and calculated the bisector spans as noted in the last column of Table 1 and plotted, as a function of RV, in Fig. 3(b). We determined S/N = 1.45 (see Christian et al. 2008 for detail), indicating no significant correlation between the bisector span and RV variations. This supports the conclusion that the motion is indeed caused by a companion planet, which, given the large RV semi-amplitude, suggests that WASP-14b is a super-massive exoplanet.

The RV residuals in Fig. 3(c) show a small dispersion of σ(O-C) = 10.1 $m\,s^{-1}$ about the MCMC fit implying a $\chi^2 = 23.62$ for 27 degrees of freedom. This is consistent with the error bars on

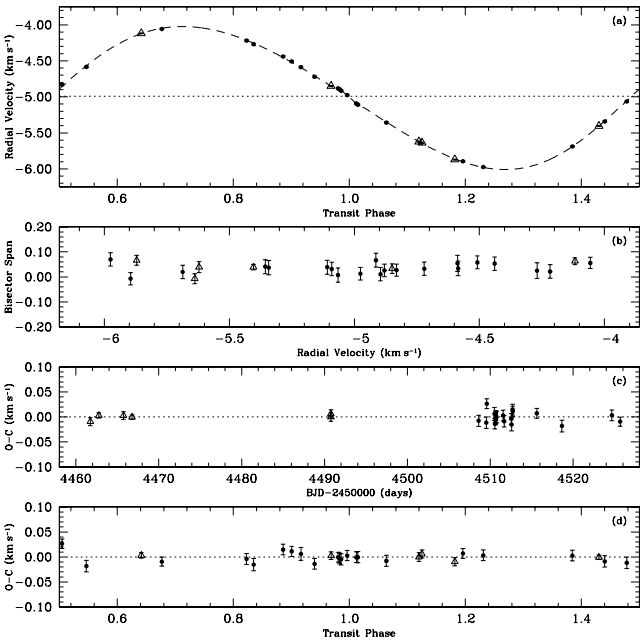

Figure 3. (a) The RV curve of WASP-14. A best-fitting MCMC model fit for the eccentric orbit is overplotted with the solid line. (b) Bisector spans as a function of RV. Residual about the MCMC fit as a function of transit phase (c), and as a function of time (d). The open triangle and filled circles are observations from the FIES and SOPHIE, respectively.

RV measurements. We note that this is also the order of magnitude of expected stellar 'jitter' in the F5 dwarf host (see e.g. Santos et al. 2000; Wright 2005). We have not noted any systematic variation in the RV residuals during two months of our observations (see Fig. 3d), and hence do not suggest the presence of any third body in the system on the basis of present data.

2.4 Rossiter–McLaughlin effect

Several RV observations were secured with SOPHIE during a transit of WASP-14b on the night of 2008 February 13. The relatively high impact parameter of the system breaks the degeneracy between $v \sin i$ and the angle λ between the projected spin axes of the rotation axis of the star and the orbit of the planet on the sky. We treated both these quantities as fitting parameters in the MCMC code, and verified that they were indeed uncorrelated. The resulting $v \sin i = 4.7 \pm 1.5\,km\,s^{-1}$, determined from the apparent radial acceleration during the transit, is consistent with $v \sin i = 4.9 \pm 1.0\,km\,s^{-1}$ derived from the spectroscopic analysis and $v \sin i = 3.0 \pm 1.5\,km\,s^{-1}$ from the width of the CCF of the SOPHIE spectra which is calibrated following the method of Santos et al. (2002). We note here that FIES spectra and SOPHIE CCF provide a $v \sin i$ averaged over all the stellar disc, whereas the Rossiter–McLaughlin (RM) fit provides the $v \sin i$ at the impact parameter of the transiting planet. The value of misalignment angle, $\lambda = -14^{+21}_{-13}$ deg, derived from the asymmetry of the RM effect, is consistent with zero obliquity, but is of insufficient precision to rule out a substantial misalignment of the stellar spin and planetary orbital axes.

An enlarged plot of RV variations around the transit phase is drawn in Fig. 4. A continuous line is overplotted for our best fit ($v \sin i = 4.7\,km\,s^{-1}$, $\lambda = -14^{\circ}$). We also overplot Keplerian fit by the dashed line determined from the RV measurements outside the transit in order not to be affected by the uncertainties of the RM

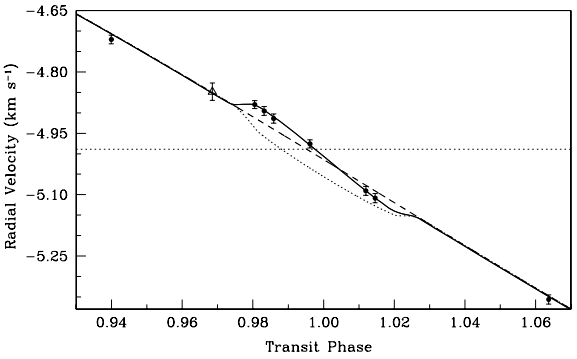

Figure 4. The RV variations around the transit phase. Solid line shows best-fitting model fit, dashed line shows Keplerian model without Rositter–McLaughlin effect and the dotted line shows the model fit of a transverse transit ($\lambda = 90^\circ$).

effect. One can see that the first four measurements performed in the first half of the transit are redshifted by comparison to the Keplerian fit, whereas the last two measurements performed in the second half of the transit are blueshifted by comparison to the Keplerian fit. The ordinary feature for an aligned, prograde transit shows that the RM anomaly is indeed significantly detected. A model of a transverse transit drawn by dotted line in the same plot clearly excludes any variations due to $\lambda = 90^\circ$. A possible transverse transit has been detected in the case of XO-3b (Hébrard, Bouchy & Pont 2008), whereas HD 147506b (HAT-P-2b) shows aligned transits (Winn et al. 2007; Loeillet et al. 2008). This suggests that the history of WASP-14b is more similar to HAT-P-2b than the other massive planet XO-3b. Given the high eccentricity of the system, it would be interesting to make further, more densely sampled observations of the RM effect in this system. This will also allow us to better constrain the system parameters, such as λ.

3 DETERMINATION OF SYSTEM PARAMETERS

3.1 $T_{\rm eff}$ from the IRFM

We used archival TYCHO, DENIS and Two-Micron All-Sky Survey (2MASS) magnitudes to estimate the host star's effective temperature using the infrared flux method (IRFM) (Blackwell & Shallis 1977). IRFM yields a nearly model-independent determination of $T_{\rm eff}$ from the integrated stellar flux. We individually estimated $T_{\rm eff}$ for J, H and K bands and a weighted mean was determined for the final value of $T_{\rm eff}$. In the case of WASP-14, we find $T_{\rm eff} = 6480 \pm 140$ K. It should be noted that no extinction correction was applied in the IRFM fitting since the star is relatively nearby and out of the Galactic plane. The $J - H = 0.22$ and $V - K = 1.13$ colours also suggest similar estimates for $T_{\rm eff}$ of ∼6230 and 6440 K, respectively (Martin 2007). This suggests the star is of spectral type of F5-7. We also determined an average angular diameter of $\theta = 0.075 \pm 0.004$ mas from the IRFM.

3.2 Spectral analysis

In order to perform a detailed spectroscopic analysis of the stellar atmospheric properties of WASP-14, we followed the same methodology as described in Pollacco et al. (2008). Our results from the spectral analysis are consistent with a F5 spectral-type main-sequence star, in agreement with the F5-7 type determined from infrared data, and the F5 type listed in SIMBAD from the PPM catalogue. In addition, we also analysed a small region around the Li I 6708 line to determine a lithium abundance that is defined as $\log N(\mathrm{Li}) \equiv 12 + (\mathrm{Li/H})$ and estimated to be 2.84. The resulting parameters from our spectral analysis are given in Table 2.

Table 2. Stellar parameters for WASP-14. The last six parameters are derived from the spectral analysis of the FIES data.

RA (2000)	$14^{\rm h}\ 33^{\rm m}\ 06.35^{\rm s}$
Dec. (2000)	$+21^\circ\ 53'\ 40.9''$
V (mag)	9.75
$B - V$ (mag)	0.46 ± 0.03
Age (Gyr)	∼0.5–1.0
Distance (pc)	160 ± 20
Spectral type	F5V
$v \sin i$ (km s^{-1})	4.9 ± 1.0
$T_{\rm eff}$ (K)	6475 ± 100
$\log g$ (cgs)	4.07 ± 0.2
[M/H] (dex)	0.0 ± 0.2
$\log N$(Li)	2.84 ± 0.05

3.3 Model fit to determine planetary parameters

Transit photometry combined with RV measurements provides detailed information about the planetary orbit and the stellar and planetary parameters. High-precision photometric data were combined with the SOPHIE RV measurements in a simultaneous MCMC analysis to find the parameters of the WASP-14 system and their covariance matrix. Our implementation of MCMC for the transiting exoplanets is presented in detail in Collier Cameron et al. (2007), with an extension to fit eccentric orbits described in Pollacco et al. (2008). Various parameters determined from the model fit along with the corresponding 1σ error limits are listed in Table 3. Since a zero eccentricity orbit is expected for such a short-period planet system due to a relatively small tidal circularization timescale (see Section 4.2), we have also analysed the model assuming a zero-eccentricity orbit which has increased χ^2 by about 370. Using the stellar radius given in the table and angular diameter of the star determined from the IRFM, we estimated a distance of about 160 ± 20 pc for the host star.

4 EVOLUTIONARY STATUS

4.1 Stellar and planetary evolution

We estimated the age of WASP-14 using a maximum-likelihood fit to the stellar evolutionary tracks for the low- and intermediate-mass stars given by Girardi et al. (2000). In Fig. 5, we have shown the position of WASP-14 in the $R/M^{1/3}$ versus $T_{\rm eff}$ plane. The evolutionary tracks of different stellar mass along with the isochrones of different ages taken from Girardi et al. (2000) models are also drawn. This shows that the star with $T_{\rm eff} = 6475 \pm 100$ K and a radius of $1.30 \pm 0.07\,{\rm R}_\odot$ is consistent with being a main-sequence object and has an interpolated mass of $1.21\,{\rm M}_\odot$ from the models. The MCMC fit to the photometry and RVs (Table 3) was computed using this value for the stellar mass, ensuring consistency between the evolutionary status and the system parameters obtained from the MCMC fit. The resulting value of $\log g = 4.33 \pm 0.06$ is higher but more precisely determined than that obtained from the spectral fit, and is consistent within the uncertainty of the latter measurement.

Table 3. Planetary and stellar parameters for the WASP-14 system derived from the MCMC analysis along with 1σ limits.

Parameter	Symbol	Values
Transit epoch (HJD)	T_0	$2454\,463.575\,83 \pm 0.000\,53$ d
Orbital period	P	$2.243\,752 \pm 0.000\,010$ d
Transit duration	T	$0.1275^{+0.0028}_{-0.0031}$ d
Transit depth	$(R_P/R_*)^2$	$0.0102^{+0.0002}_{-0.0003}$ mag
Impact parameter	b	$0.535^{+0.031}_{-0.041}$ $R_\odot$
Orbital inclination	i	$84.32^{+0.67}_{-0.57}$ deg
Orbital semimajor axis	a	0.036 ± 0.001 au
Orbital eccentricity	e	0.091 ± 0.003
Arg. periastron	ω	$-106.629^{+0.693}_{-0.678}$ rad
Stellar reflex velocity	K_1	0.993 ± 0.003 km s^{-1}
Centre-of-mass velocity	γ	-4.990 ± 0.002 km s^{-1}
Stellar mass	M_*	$1.211^{+0.127}_{-0.122}$ $M_\odot$
Stellar radius	R_*	$1.306^{+0.066}_{-0.073}$ $R_\odot$
Stellar density	ρ_*	$0.542^{+0.079}_{-0.060}$ $\rho_\odot$
Stellar surface gravity	$\log g_*$	$4.287^{+0.043}_{-0.038}$ (cgs)
Planet mass	M_P	$7.341^{+0.508}_{-0.496}$ M_J
Planet radius	R_P	$1.281^{+0.075}_{-0.082}$ R_J
Planet density	ρ_P	$3.501^{+0.636}_{-0.495}$ ρ_J
Planetary surface gravity	$\log g_P$	$4.010^{+0.049}_{-0.042}$ (cgs)
Planet temp ($A = 0$)	T_P	$1866.12^{+36.74}_{-42.09}$ K
Photometric data points	N_{df}	6482
χ^2 (photometric)	χ^2_{phot}	6452.78
Spectroscopic data points	N_{df}	27
χ^2 (spectroscopic)	χ^2_{spec}	23.62

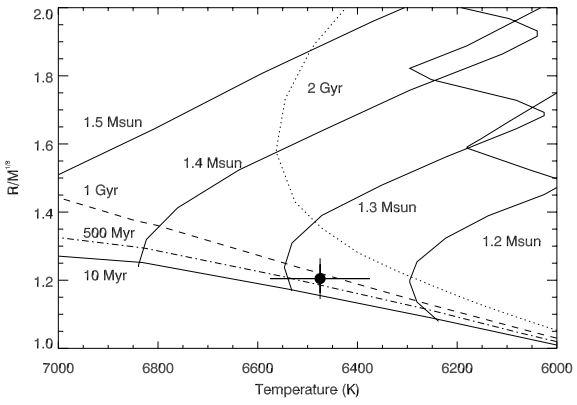

Figure 5. Position of WASP-14 in $R/M^{1/3} - T_{\rm eff}$ plane. Girardi et al. (2000) solar metallicity stellar evolutionary tracks for different masses and isochrones of different ages are also shown.

Although there is a significant uncertainty in the effective temperature of the star, WASP-14 seems to be consistent with being an approximate age of 0.5–1.0 Gyr.

In F-type stars, the convection zone does not penetrate deep enough to transport lithium to the regions with temperatures above 6000 K, reducing the efficiency of lithium depletion, with the exception of the Li gap or 'Boesgaard gap' (Boesgaard & Tripicco 1986; Balachandran 1995). The temperature of WASP-14, $T_{\rm eff} = 6475 \pm 100$ K, places it close to the Li gap, where lithium depletion is enhanced by an as-yet unknown mechanism (Böhm-Vitense 2004). Although the rate of lithium depletion in the Li gap is not very well calibrated, the relatively high lithium content, $\log N({\rm Li}) = 2.84 \pm 0.05$, and rotation speed, $v \sin i = 4.9 \pm 1.0$ km s^{-1}, possibly indicate that WASP-14 is a young star. Similar high levels of lithium are also found in the Hyades cluster (age ~ 600 Myr) with $\log N({\rm Li}) = 2.77 \pm 0.21$ for the stars with $T_{\rm eff} = 6200 \pm 150$ K (Sestito & Randich 2005).

We further compare our results with the models of Fortney et al. (2007) where masses and radii are given for a range of planetary masses, orbital separations and stellar ages. For WASP-14b, these models predict a planetary radius <1.20 R_J for a host star of age 1 Gyr, while for an age of 300 Myr, the radius is predicted to be about 1.20–1.26 R_J. A radius of 1.28 ± 0.08 R_J for the planet suggests that WASP-14 possibly lies somewhere in the middle of these two age limits – in agreement with our earlier finding. For massive planets ($>5M_J$), the model shows <3 per cent change in planet radius with the cores of mass from 0 to $100M_\oplus$. In the context of Fortney et al. (2007) model, our observations do not place strong constraints on the core mass of WASP-14b.

4.2 Tidal evolution

One of the interesting features of WASP-14b is its high orbital eccentricity, $e = 0.091$, for its small orbital distance of 0.036 au. At this distance, any orbital eccentricity should induce strong tidal energy dissipation within the planet leading to circularization of the orbit. Matsumura, Takeda & Rasio (2008) determined a median eccentricity of 0.013 for close-in planets with semimajor axis $a <$ 0.1 au. The nearly circular orbits of most close-orbiting exoplanets indicate tidal circularization time-scales significantly shorter than the system age. The high eccentricity of WASP-14b may thus indicate either a system age comparable to the tidal circularization time-scale or the presence of an additional perturbing body in the system.

In the tidal evolution scenario originally developed by Goldreich & Soter (1966) and more recently discussed by Dobbs-Dixon, Lin & Mardling (2004), Jackson, Greenberg & Barnes (2008) and others, the circularization time-scale (τ_e) and spiral-in time-scale (τ_a) for a single planet are given by the logarithmic time derivatives of the orbital eccentricity and semimajor axis:

$$\tau_e = e/\dot{e}; \quad \tau_a = a/\dot{a}.$$

Using the equations given in Jackson et al. (2008) for close-in extrasolar planets, and the planetary and stellar parameters for the WASP-14 system, we obtain $\tau_e \simeq 1/[28.5/(Q_{\rm p}/10^5) + 6.6/(Q_{\rm s}/10^6)]$ Gyr and $\tau_a \simeq 1/[0.5165(e/0.089)^2/(Q_{\rm p}/10^5) + 2.359/(Q_{\rm s}/10^6)]$ Gyr. Here, the tidal dissipation parameters $Q_{\rm p}$ for the planet and $Q_{\rm s}$ for the star are assigned fiducial values of 10^5 and 10^6, respectively, in accordance with the best-fitting values derived from the study of Jackson et al. (2008). It should be mentioned here that there could be considerable uncertainties in both these parameters; moreover, the time-scales are inversely proportional to the fifth powers of the planetary and stellar radii, both of which contain significant uncertainties in their determinations.

From the expression for τ_e above, the circularization time-scale of the planet's orbit will be less than 1 Gyr if either $Q_{\rm p} < 3.7 \times 10^6$ or $Q_{\rm s} < 6.6 \times 10^6$. The time-scale for the decay of the orbital semimajor axis of the planet via torques arising from the tidal bulge raised on the star could also be less than 1 Gyr if $Q_{\rm s} < 2.4 \times 10^6$. These same torques might be expected to spin the star up on a time-scale of the order of 1 Gyr, since the angular-momentum loss in the

wind of a F star like WASP-14 is quite weak. A dissipation factor $Q_s > 6.6 \times 10^6$ could increase the life expectancy of the planet to a value similar to the main-sequence lifetime of the F-type host.

If Q_p is low and the circularization time-scale is short, the most plausible alternative mechanism for maintaining the high eccentricity of WASP-14b is secular interaction with an additional planet in the system (see e.g. Adams & Laughlin 2006). From the above arguments, however, it is not clear whether an additional planet is needed to maintain the observed eccentricity over the ∼1 Gyr lifetime of the star. This is only needed if the rate at which tidal energy is dissipated in the planet is high, with $Q_p < 3 \times 10^6$. The slow stellar spin suggests that magnetic braking is dominating over torques arising from the tidal bulge raised on the star. This in turn suggests a low rate of dissipation in the star, with $Q_s > 10^8$ or so. A further discussion of eccentric orbits in close-in exoplanets and their constraints on Q can be found in Matsumura et al. (2008).

Two other recently announced planets WASP-10b ($e = 0.059$; Christian et al. 2008) and WASP-12b ($e = 0.064$; Hebb et al. 2008) also have apparently significant orbital eccentricity. While Shen & Turner (2008) noted that the sparsely sampled RV curves are often interpreted as having significant orbital eccentricity, in the case of the WASP planets the spectroscopic data are usually obtained over a small number of cycles and with good precision. Consequently, we expect the eccentricities derived for these systems to be free from bias or selection effects.

5 DISCUSSION

We have discovered a new massive exoplanet WASP-14b orbiting with a period of about 2.244 d around its host main-sequence star GSC 01482−00882. The spectral analysis of the star implies a spectral type of F5V with solar metallicity. High-precision photometric and spectroscopic follow-up observations reveal that the planet has a mass of $7.3 \pm 0.5\ M_J$, radius of $1.28 \pm 0.08\ R_J$, suggesting a mean density of $3.5 \pm 0.6\ \rho_J$(∼4.6 g cm^{-3}), and an eccentricity of 0.091 ± 0.003. The mean density of WASP-14b is high in comparison with a typical hot Jupiter density of 0.34–1.34 g cm^{-3} (Loeillet et al. 2008), and similar to that of rocky planets and makes it the densest transiting exoplanets so far discovered with <3 d orbital period. The planet is too massive to fit the mass–period relation given by Torres, Winn & Holman (2008), but its radius is consistent with the theoretical radius expected from the Fortney et al. (2007) model. The spectral analysis reveals that WASP-14 has a high lithium abundance, $\log N(\mathrm{Li}) = 2.84$. This is consistent with its stellar temperature ($T_{\rm eff} = 6475 \pm 100$ K) and age of about 0.5–1.0 Gyr which is further supported by the fitting of stellar evolutionary models of Girardi et al. (2000).

High orbital eccentricities in close-in planets are often explained by the perturbations from a third body (Jackson et al. 2008 and references therein) or the internal structures that result in their tidal dissipation factor being significantly larger than that commonly assumed $Q_p \sim 10^6$ (Hebb et al. 2008; Matsumura et al. 2008). Although we do not see any systematic variation in RV residuals during our two months of spectroscopic observations of WASP-14, we expect that long-term RV monitoring will help constrain the nature of the third body in this systems and hence makes it an important target both for future transit-timing variation studies and for longer term RV monitoring to establish the mass and period of the putative outer planet.

WASP-14b is one of the most massive transiting planets known along with HAT-P-2b (Bakos et al. 2007; Winn et al. 2007; Loeillet et al. 2008) and XO-3b (Hébrard et al. 2008; Johns-Krull et al. 2008; Winn et al. 2008), and its physical characteristics closely resemble with those of HAT-P-2 except the latter has a much longer orbital period and smaller radius. However, there is still no firm explanation about the formation of such highly massive planets (e.g. Hébrard et al. 2008). A quite interesting feature is that all these three massive exoplanets have unusually large eccentric orbit for their short orbital period. Matsumura et al. (2008) argue that the new class of eccentric, short-period transiting planets are still in the process of circularization and speculate that Q_p could be as large as 10^9 for these planets.

The success of theoretical models of planetary structure depends heavily on our precise knowledge of the basic physical parameters of the planetary systems. Transit surveys in recent times have produced a large sample of transiting planets that show a remarkable diversity in their mass, radius and internal structure. While most of the Jupiter mass transiting planets are well explained by the existing models, planets which show excessive mass for their small radius or relatively low mass for their large radius are yet to be explained satisfactorily by any available model. WASP-14b is one of the few massive exoplanets, some of which are even in closer orbits than most other hot Jupiters. It poses a great challenge for theoretical models to explain their internal structure, atmospheric dynamics and heat distribution.

ACKNOWLEDGMENTS

The SuperWASP Consortium consists of astronomers primarily from the Queen's University Belfast, St Andrews, Keele, Leicester, The Open University, Isaac Newton Group La Palma and Instituto de Astrofísica de Canarias. SuperWASP Cameras were constructed and operated with funds made available from Consortium Universities and the UK's Science and Technology Facilities Council. SOPHIE observations have been funded by the Optical Infrared Coordination Network. Data from the Liverpool and NOT telescopes were obtained under the auspices of the International Time of the Canary Islands. We extend our thanks to the staff of the ING and OHP for their continued support of SuperWASP-N and SOPHIE instruments. FPK is grateful to AWE Aldermaston for the award of a William Penney Fellowship.

REFERENCES

Adams F. C., Laughlin G., 2006, ApJ, 649, 992
Bakos G. A., Noyes R. W., Kovács G., Stanek K. Z., Sasselov D. D., Domsa I., 2004, PASP, 116, 266
Bakos G. A. et al., 2007, ApJ, 670, 826
Balachandran S., 1995, ApJ, 446, 203
Blackwell D. E., Shallis M. J., 1977, MNRAS, 180, 177
Boesgaard A. M., Tripicco M. J., 1986, ApJ, 303, 724
Böhm-Vitense E., 2004, AJ, 128, 2435
Charbonneau D., Brown T. M., Latham D. W., Mayor M., 2000, ApJ, 529, L45
Christian D. et al., 2008, MNRAS, in press (arXiv0806.1482)
Collier Cameron A. et al., 2006, MNRAS, 373, 799
Collier Cameron A. et al., 2007, MNRAS, 380, 1230
Dobbs-Dixon I., Lin D. N. C., Mardling R. A., 2004, ApJ, 610, 464
Fortney J. J., Marley M. S., Barnes J. W., 2007, ApJ, 659, 1661
Gibson N. et al., 2008, A&A, in press (arXiv:0810.3526)
Girardi L., Bressan A., Bertelli G., Chiosi C., 2000, A&AS, 141, 371
Goldreich P., Soter S., 1966, Icar, 5, 375
Guillot T., Santos N. C., Pont F., Iro N., Melo C., Ribas I., 2006, A&A, 453, L21
Hebb L. et al., 2008, ApJ, submitted
Hébrard G., Bouchy F., Pont F., 2008, A&A, 488, 763

Henry G. W., Marcy G. W., Butler R. P., Vogt S. S., 2000, ApJ, 529, L41
Jackson B., Greenberg R., Barnes R., 2008, ApJ, 678, 1396
Johns-Krull C. M. et al., 2008, ApJ, 677, 657
Loeillet B. et al., 2008, A&A, 481, 529
McCullough P. R., Stys J., Valenti J., Fleming S., Janes K., Heasley J., 2005, PASP, 117, 783
Martin V. Z., 2007, Handbook of Space and Astrophysics, 3rd edn. Cambridge Univ. Press, Cambridge
Matsumura S., Takeda G., Rasio F. A., 2008, ApJ, 686, L29
O'Donovan F. T. et al., 2006, ApJ, 651, L61
Pollacco D. et al., 2006, PASP, 118, 1407
Pollacco D. et al., 2008, MNRAS, 385, 1576
Queloz D. et al., 2001, A&A, 379, 279
Santos N. C., Mayor M., Naef D., Pepe F., Queloz D., Urdy S., Blecha A., 2000, A&A, 361, 265
Santos N. C., Mayor M., Naef D., Pepe F., Queloz D., Urdy S., Burnet M., Revaz Y., 2002, A&A, 392, 215,
Sestito P., Randich S., 2005, A&A, 442, 615
Shen Y., Turner E. L., 2008, ApJ, 685, 553
Steele I., Bates S. D., Gibson N., Keenan F., Meaburn J., Mottram C. J., Pollaco D., Todd I., 2008, in McLean I. S., Casali M. M. eds, Proc. SPIE, Vol. 7014, Ground-based and Airborne Instrumentation for Astronomy II. SPIE, Bellingham, p. 70146
Torres G., Winn J. N., Holman M., 2008, ApJ, 677, 1324
Winn J. N. et al., 2007, ApJ, 665, L167
Winn J. N. et al., 2008, ApJ, 683, 1076
Wright J. T., 2005, PASP, 117, 657

This paper has been typeset from a TEX/LATEX file prepared by the author.